

Electronic Supplementary Information

For

**Highly efficient solution-processed pure yellow OLED based on dinuclear Pt(II) complexes**

Yuanhui Sun,<sup>a</sup> Bochen Liu,<sup>b</sup> Bo Jiao,<sup>c</sup> Yue Guo,<sup>b</sup> Xi Chen,<sup>a</sup> Guijiang Zhou,<sup>\*a</sup> Zhao Chen<sup>\*b</sup> and Xiaolong Yang<sup>\*a</sup>

<sup>a</sup> School of Chemistry, MOE Key Laboratory for Nonequilibrium Synthesis and Modulation of Condensed Matter, Xi'an Key Laboratory of Sustainable Energy Material Chemistry, Xi'an Jiaotong University, Xi'an 710049, P. R. China.

E-mail: zhougj@xjtu.edu.cn, xiaolongyang@xjtu.edu.cn

<sup>b</sup> School of Applied Physics and Materials, Wuyi University, Jiangmen 529020, P. R. China.

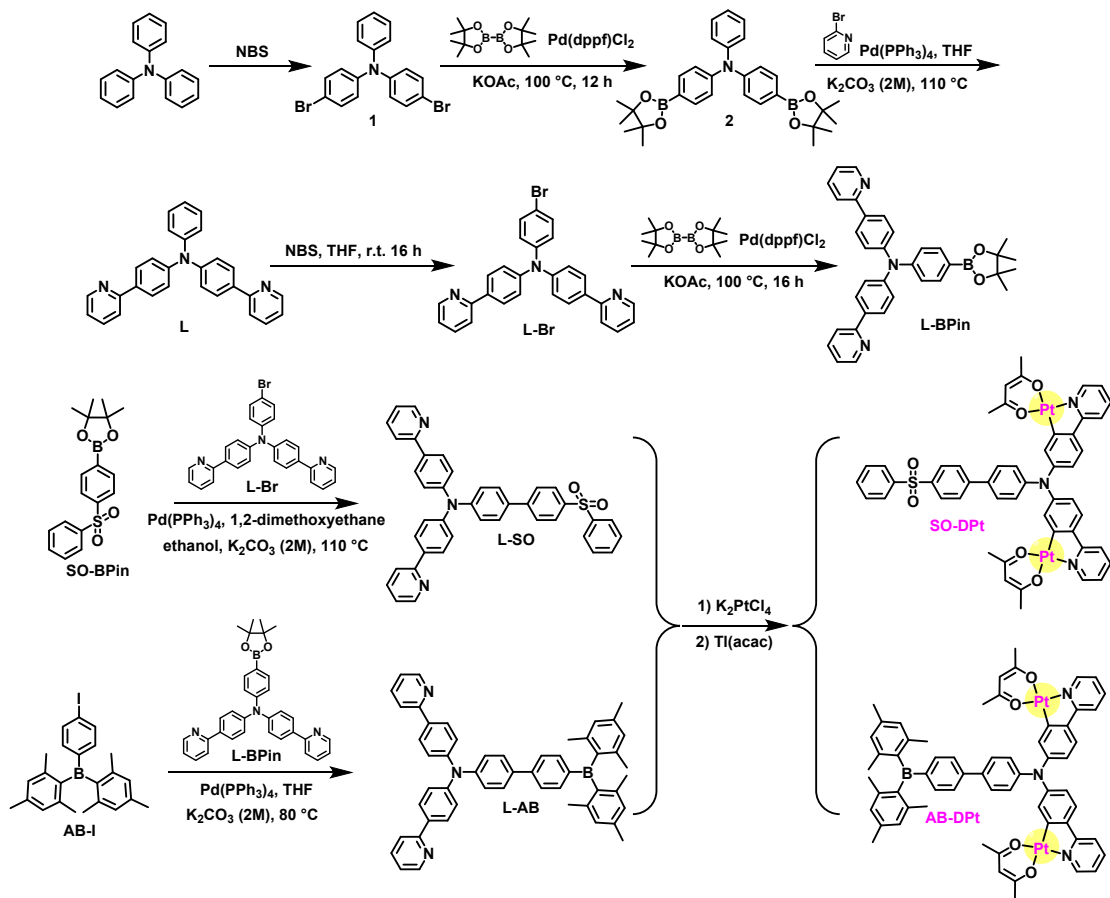
E-mail: chenzhao2006@163.com

<sup>c</sup> School of Electronic and Information Engineering, Key Laboratory for Physical Electronics and Devices of the Ministry of Education, Shaanxi Key Lab of Information Photonic Technique, Xi'an Jiaotong University, Xi'an 710049, P. R. China.

## General Information

Commercially available reagents were used directly without further purification. NMR spectra ( $^1\text{H}$  and  $^{13}\text{C}$ ) were recorded on a Bruker Avance 400 MHz spectrometer in  $\text{CDCl}_3$ . Mass spectra were measured on the WATERS I-Class VION IMS Qtof mass spectroscopy. The thermal gravimetric analysis (TGA) was studied with a NETZSCH STA 409C instrument under  $\text{N}_2$  at a heating rate of 20 K/min. UV-vis absorption spectra of Pt(II) complexes in  $\text{CH}_2\text{Cl}_2$  solutions at a concentration of *ca.*  $3 \times 10^{-5}$  M were measured on a Shimadzu UV-2250 spectrophotometer at room temperature. Photoluminescent spectra and lifetimes of Pt(II) complexes in doped films were measured on an Edinburgh Instruments Ltd (FLSP920) fluorescence spectrophotometer. The PLQYs of doped films were tested with an integrating sphere. Cyclic voltammetry curves were recorded with a Princeton Applied Research equipment (PARSTAT 2273) in  $\text{CH}_2\text{Cl}_2$  solutions using *n*-Bu<sub>4</sub>NPF<sub>6</sub> (0.1 M) as the supporting electrolyte and ferrocene/ferrocenium (Fc/Fc<sup>+</sup>) couple as the reference. Energy levels of HOMOs ( $E_{\text{HOMO}}$ ) were determined from the onset of oxidation potentials ( $E_{\text{ox}}$ ) according to  $E_{\text{HOMO}} = -(E_{\text{ox}} + 4.8)$  eV and energy levels of LUMOs ( $E_{\text{LUMO}}$ ) were determined from  $E_{\text{LUMO}} = -(E_{\text{red}} + 4.8)$  eV. Theoretical computations based on density functional theory (DFT) and time dependent-DFT (TD-DFT) were carried out for all three dinuclear Pt(II) complexes with Gaussian 09 program. Non-metal atoms of C, H, N, O, S, and B were described by the basis set of B3LYP/6-31G(d, p). The metal atom Pt was described by the B3LYP/LanL2DZ basis set.

**OLED Fabrication and Measurements.** The ITO glass substrates were pre-cleaned in ultrasonic cleaner with detergent and deionized water. The substrates were treated with UV-O<sub>3</sub> for 30 minutes before use. Then, PEDOT:PSS was spin-coated on the surface of ITO glass substrates to form a hole-injection layer and annealed at 150 °C for 15 min in the air. The hole transport layer was prepared by spin-coating the chlorobenzene solution of PVK on the surface of PEDOT:PSS layer and annealed at 120 °C for 10 min in a glove box. After spin-coating the chlorobenzene solution of Pt(II) complexes and CBP host (1, 2, or 3 wt% doping level) to form the emissive layer, the TmPyPB (40 nm), LiF 1 (nm), and Al (100 nm) layers were vucuum deposited under a pressure of  $5 \times 10^{-4}$  torr. The current density-voltage (*I*-*V*) curves were measured by a SourceMeter (Keithely 2400). The EL spectra and luminance values were measured with a PR788 spectra colorimeter. The efficiency and spectra tests were carried out under ambient conditions.



**Scheme S1** Synthetic routes of dinuclear Pt(II) complexes.

**Compound 1:** To a solution of triphenylamine (2.45 g, 10.0 mmol) in CHCl<sub>3</sub> (30 mL) at 0 °C, *N*-bromosuccinimide (NBS, 3.56 g, 20.0 mmol) was added very slowly. Then the mixture was stirred at room temperature overnight. After being washed with water, the organic layer was separated, dried over anhydrous MgSO<sub>4</sub>, and concentrated with a rotary evaporator. The residual was purified on a silica column using petroleum ether as the eluent to the target product (3.71 g, 92% yield). <sup>1</sup>H NMR (400 MHz, CDCl<sub>3</sub>, δ): 7.37–7.31 (m, 4H), 7.29–7.24 (m, 2H), 7.08–7.03 (m, 3H), 6.96–6.92 (m, 4H).

**Compound 2:** The mixture of compound 1 (2.02 g, 5.0 mmol), bis(pinacolato)diboron (2.86 g, 11.0 mmol), Pd(dppf)Cl<sub>2</sub> (0.48 g, 0.66 mmol), and potassium acetate (3.30 g, 33.7 mmol) were added to dioxane (50 mL) and stirred at

100 °C for 12 h under a N<sub>2</sub> atmosphere. After cooled to room temperature, the mixture was poured into water and extracted with CH<sub>2</sub>Cl<sub>2</sub> several times. The organic layers were combined, dried over anhydrous MgSO<sub>4</sub> and concentrated with a rotary evaporator. The residual was purified on a silica column using a mixture of petroleum ether and CH<sub>2</sub>Cl<sub>2</sub> as the eluent to give the target product (1.67 g, 67 % yield). <sup>1</sup>H NMR (400 MHz, CDCl<sub>3</sub>, δ): 7.67 (d, *J* = 8.0 Hz, 4H), 7.28–7.24 (m, 3H), 7.11 (d, *J* = 8.4 Hz, 2H), 7.06 (d, *J* = 8.4 Hz, 4H), 1.33 (s, 24H); <sup>13</sup>C NMR (100 MHz, CDCl<sub>3</sub>, δ): 150.10, 147.02, 135.86, 129.35, 125.58, 124.96, 123.86, 122.71, 83.60, 24.84.

**Compound L:** Under a N<sub>2</sub> atmosphere, the mixture of compound **2** (1.0 g, 2.0 mmol), 2-bromopyridine (0.66 g, 4.2 mmol), and Pd(PPh<sub>3</sub>)<sub>4</sub> (0.24 g, 0.21 mmol) were stirred in the THF (30 mL) and 2 M K<sub>2</sub>CO<sub>3</sub> (20 mL) at 110 °C overnight. The reaction mixture was cooled to room temperature, poured into water, and extracted with CH<sub>2</sub>Cl<sub>2</sub> several times. The organic layers were combined, dried over anhydrous MgSO<sub>4</sub> and concentrated with a rotary evaporator. The residual was purified on a silica column using a mixture of petroleum ether and CH<sub>2</sub>Cl<sub>2</sub> as the eluent to give the related target product (0.69 g, 86.8% yield). <sup>1</sup>H NMR (400 MHz, CDCl<sub>3</sub>, δ): 8.66 (d, *J* = 4.4 Hz, 2H), 7.90 (d, *J* = 8.8 Hz, 4H), 7.75–7.67 (m, 4H), 7.30 (t, *J* = 8.0 Hz, 2H), 7.25–7.17 (m, 8H), 7.09 (t, *J* = 7.2 Hz, 1H); <sup>13</sup>C NMR (100 MHz, CDCl<sub>3</sub>, δ): 156.99, 149.60, 148.28, 147.15, 136.66, 133.68, 129.40, 127.81, 125.15, 123.85, 123.67, 121.55, 119.95.

**Compound L-Br:** To a solution of compound L (1.0 g, 2.5 mmol) in THF (100 mL) at room temperature, *N*-bromosuccinimide (NBS, 0.46 g, 2.6 mmol) was added very slowly. Then the mixture was stirred overnight. After being washed with water,

the organic layer was separated, dried over anhydrous  $\text{MgSO}_4$ , and concentrated with a rotary evaporator. The residual was purified on a silica column using the mixture of  $\text{CH}_2\text{Cl}_2$  and ethyl acetate as the eluent to the target product (1.16 g, 97.2% yield).  $^1\text{H}$  NMR (400 MHz,  $\text{CDCl}_3$ ,  $\delta$ ): 8.66 (d,  $J = 4.8$  Hz, 2H), 7.90 (d,  $J = 8.8$  Hz, 4H), 7.75–7.67 (m, 4H), 7.38 (dd,  $J = 5.2, 7.2$  Hz, 2H), 7.21–7.18 (m, 6H), 7.05 (d,  $J = 8.8$  Hz, 2H);  $^{13}\text{C}$  NMR (100 MHz,  $\text{CDCl}_3$ ,  $\delta$ ): 156.78, 149.61, 147.74, 146.27, 136.70, 134.18, 132.35, 127.93, 126.12, 124.06, 121.68, 119.99, 115.91.

**Compound L-BPin:** The mixture of compound **L-Br** (1.1 g, 2.3 mmol), bis(pinacolato)diboron (0.89 g, 3.5 mmol),  $\text{Pd}(\text{dpff})\text{Cl}_2$  (0.17 g, 0.23 mmol), and potassium acetate (1.1 g, 11.2 mmol) were added to dioxane (35 mL). The reaction mixture was stirred at 100 °C for 16 h under a  $\text{N}_2$  atmosphere. After cooled to room temperature, the mixture was poured into water and extracted with  $\text{CH}_2\text{Cl}_2$  several times. The organic layers were combined, dried over anhydrous  $\text{MgSO}_4$  and concentrated with a rotary evaporator. The residual was purified on a silica column using a mixture of petroleum ether and ethyl acetate as the eluent to give the target product (0.8 g, 66.2% yield).  $^1\text{H}$  NMR (400 MHz,  $\text{CDCl}_3$ ,  $\delta$ ): 8.66 (d,  $J = 4.8$  Hz, 2H), 7.90 (d,  $J = 8.4$  Hz, 4H), 7.74–7.67 (m, 6H), 7.23 (d,  $J = 8.8$  Hz, 4H), 7.20–7.15 (m, 4H), 1.34 (s, 12H);  $^{13}\text{C}$  NMR (100 MHz,  $\text{CDCl}_3$ ,  $\delta$ ): 156.76, 149.75, 149.49, 147.77, 136.66, 135.91, 134.15, 127.83, 124.52, 122.88, 121.61, 120.00, 83.58, 24.78.

Compounds **SO-BPin** and **AB-I** were synthesized according to our previous studies.<sup>1,2</sup>

**Compound L-SO:** Under a N<sub>2</sub> atmosphere, the mixture of compound **SO-BPin** (0.42 g, 1.2 mmol), **L-Br** (0.48 g, 1.0 mmol), and Pd(PPh<sub>3</sub>)<sub>4</sub> (0.07 g, 0.06 mmol) were stirred in the 1,2-dimethoxyethane (20 mL), ethanol (5 mL), and 2 M K<sub>2</sub>CO<sub>3</sub> (15 mL) at 110 °C overnight. The reaction mixture was cooled to room temperature, poured into water, and extracted with CH<sub>2</sub>Cl<sub>2</sub> several times. The organic layers were combined, dried over anhydrous MgSO<sub>4</sub> and concentrated with a rotary evaporator. The residual was purified on a silica column using a mixture of petroleum ether and ethyl acetate as the eluent to give the related target product (0.4 g, 65.0% yield). <sup>1</sup>H NMR (400 MHz, CDCl<sub>3</sub>, δ): 8.67 (d, *J* = 4.4 Hz, 2H), 7.98 (d, *J* = 7.2 Hz, 4H), 7.93 (d, *J* = 8.4 Hz, 4H), 7.76–7.69 (m, 6H), 7.58–7.48 (m, 6H), 7.26–7.12 (m, 7H); <sup>13</sup>C NMR (100 MHz, CDCl<sub>3</sub>, δ): 156.83, 149.66, 147.76, 145.45, 139.52, 136.73, 134.48, 133.30, 133.11, 132.03, 129.28, 128.24, 128.18, 128.00, 127.60, 127.30, 124.55, 124.25, 121.75, 120.06.

**Compound L-AB:** Under a N<sub>2</sub> atmosphere, the mixture of **AB-I** (0.4 g, 0.88 mmol), **L-BPin** (0.4 g, 0.76 mmol), and Pd(PPh<sub>3</sub>)<sub>4</sub> (0.051 g, 0.04 mmol) were stirred in the THF (25 mL) and 2 M K<sub>2</sub>CO<sub>3</sub> (15 mL) at 80 °C for 5 h. The reaction mixture was cooled to room temperature, poured into water, and extracted with CH<sub>2</sub>Cl<sub>2</sub> several times. The organic layers were combined, dried over anhydrous MgSO<sub>4</sub> and concentrated with a rotary evaporator. The residual was purified on a silica column using a mixture of ethyl acetate and CH<sub>2</sub>Cl<sub>2</sub> as the eluent to give the related target product (0.25 g, 45.5% yield). <sup>1</sup>H NMR (400 MHz, CDCl<sub>3</sub>, δ): 8.69 (d, *J* = 4.4 Hz, 2H), 7.95 (d, *J* = 8.8 Hz, 4H), 7.78–7.71 (m, 4H), 7.63–7.61 (m, 6H), 7.29–7.26 (m, 6H), 7.22 (t, *J* = 5.6 Hz, 2H), 6.86 (s, 4H), 2.34 (s, 6H), 2.07 (s, 12H); <sup>13</sup>C NMR (100 MHz, CDCl<sub>3</sub>, δ): 156.91, 149.63, 147.99, 146.95, 143.57, 140.81, 138.54, 137.17, 136.69,

135.37, 134.06, 128.14, 128.07, 127.90, 126.02, 124.76, 124.20, 121.64, 119.99, 23.47, 21.22.

**General procedure for synthesizing dinuclear Pt(II) complexes:** Under a N<sub>2</sub> atmosphere, the mixture solution of 2-ethoxyethanol and H<sub>2</sub>O (3:1, v/v) (25 mL), organic ligand (1.0 equiv), and K<sub>2</sub>PtCl<sub>4</sub> (ca. 2.1 equiv) were stirred at 90 °C for 4 h. After cooled to room temperature, the mixture was extracted with CH<sub>2</sub>Cl<sub>2</sub> several times. The collected organic layers were dried over anhydrous MgSO<sub>4</sub> and concentrated with a rotary evaporator. Then, the residual was mixed with thallium(I) acetylacetone (ca. 2.1 equiv) in CH<sub>2</sub>Cl<sub>2</sub> (20 mL), and stirred at room temperature overnight under a N<sub>2</sub> atmosphere. Finally, the solvent was removed, and the residual was purified on self-made silica TLC to give the target dinuclear Pt(II) complexes.

**SO-DPt** (19.2% yield). <sup>1</sup>H NMR (400 MHz, CDCl<sub>3</sub>, δ): 8.93 (d, *J* = 5.6 Hz, 2H), 8.01–7.98 (m, 4H), 7.77 (t, *J* = 7.6 Hz, 2H), 7.70 (d, *J* = 8.4 Hz, 2H), 7.60–7.50 (m, 7H), 7.39–7.35 (m, 6H), 7.05 (t, *J* = 6.4 Hz, 2H), 6.93 (d, *J* = 8.0 Hz, 2H), 5.40 (s, 2H), 1.99 (s, 6H), 1.75 (s, 6H); <sup>13</sup>C NMR (100 MHz, CDCl<sub>3</sub>, δ): 185.62, 184.13, 167.72, 148.03, 147.47, 147.17, 145.92, 141.90, 139.86, 139.40, 139.14, 137.94, 133.06, 132.82, 129.26, 128.18, 127.75, 127.59, 127.17, 125.36, 125.21, 123.99, 120.14, 119.78, 117.89, 102.36, 28.22, 26.96; ESI-MS (*m/z*) theoretical [M]<sup>+</sup>: 1201.20, found: 1201.20.

**AB-DPt** (18.9 % yield). <sup>1</sup>H NMR (400 MHz, CDCl<sub>3</sub>, δ): 8.90 (d, *J* = 5.2 Hz, 2H), 7.73 (t, *J* = 7.2 Hz, 2H), 7.58–7.56 (m, 6H), 7.49 (d, *J* = 8.0 Hz, 2H), 7.38–7.32 (m, 6H), 7.01 (t, *J* = 6.0 Hz, 2H), 6.92 (dd, *J* = 6.0, 8.4 Hz, 2H), 6.83 (s, 4H), 5.38 (s, 2H),

2.32 (s, 6H), 2.04 (s, 12H), 1.96 (s, 6H), 1.74 (s, 6H);  $^{13}\text{C}$  NMR (100 MHz,  $\text{CDCl}_3$ ,  $\delta$ ): 185.53, 184.24, 167.84, 165.03, 147.70, 147.15, 144.25, 143.79, 140.80, 139.78, 138.99, 138.46, 137.87, 137.18, 135.08, 128.12, 127.73, 126.03, 125.83, 124.92, 123.93, 119.98, 119.45, 117.82, 102.32, 28.22, 26.96, 23.48, 21.22; ESI-MS ( $m/z$ ) theoretical  $[\text{M}]^+$ : 1309.38, found: 1309.38.

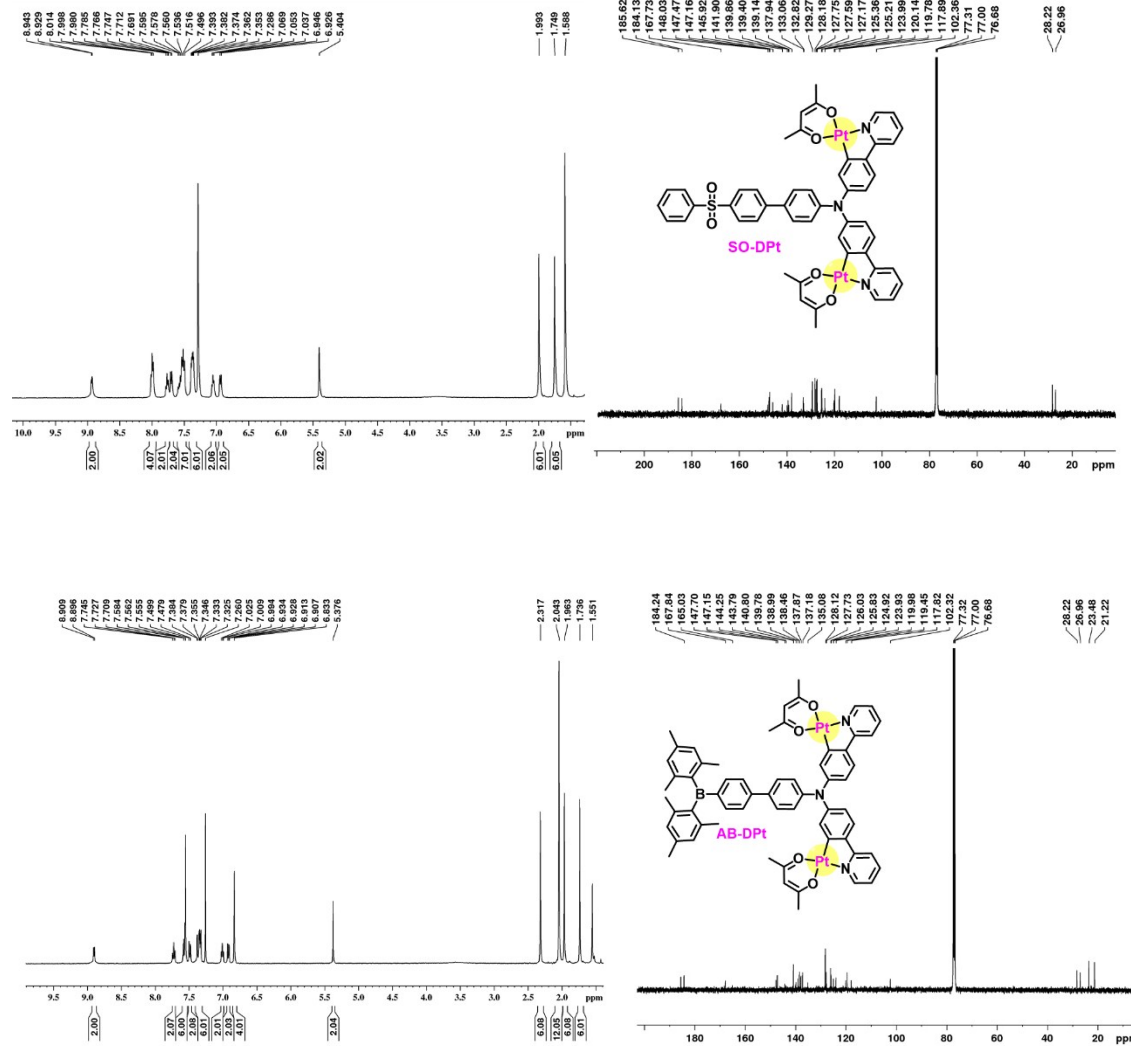


**Fig. S1** NMR spectra of **SO-DPt** and **AB-DPt**.

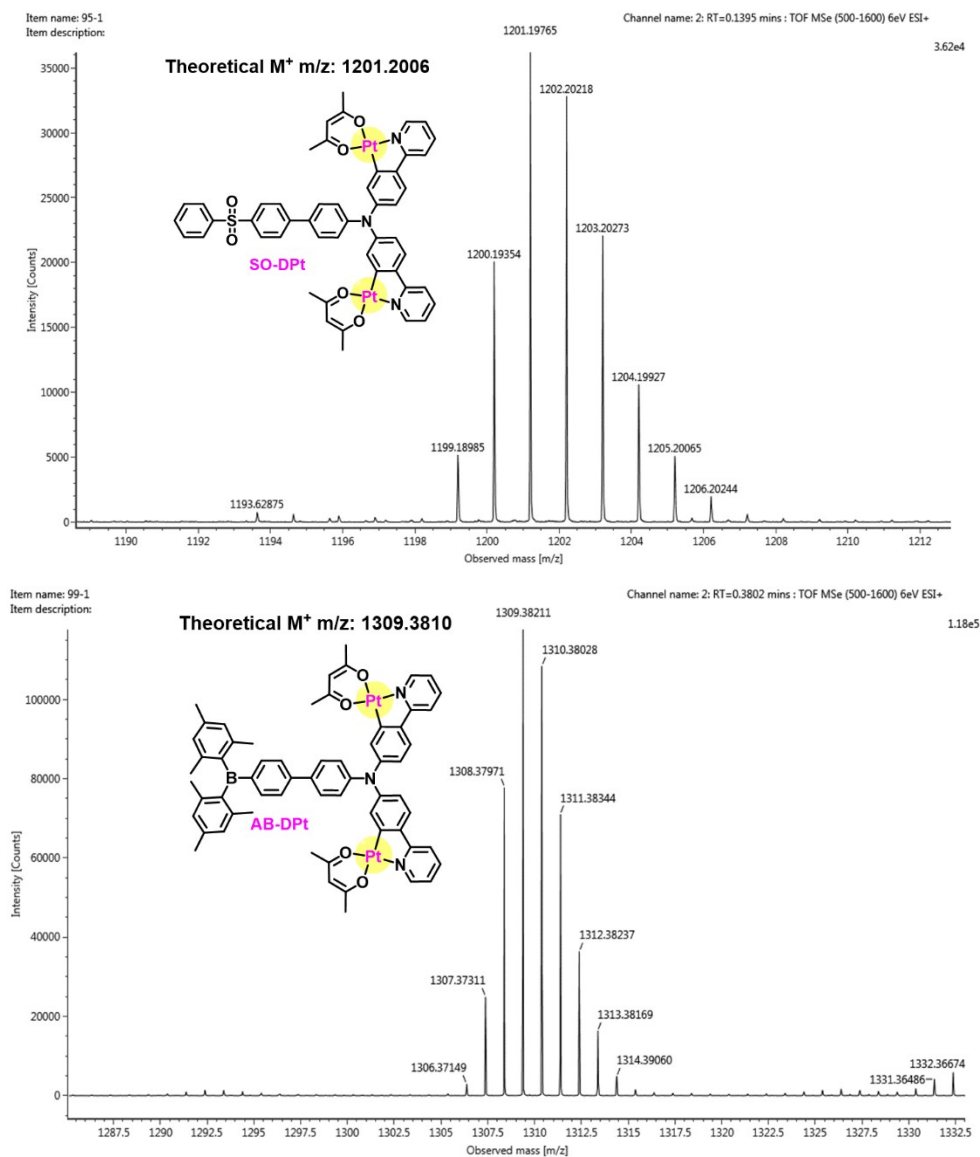


**Fig. S2** Mass spectra of SO-DPt and AB-DPt complexes.

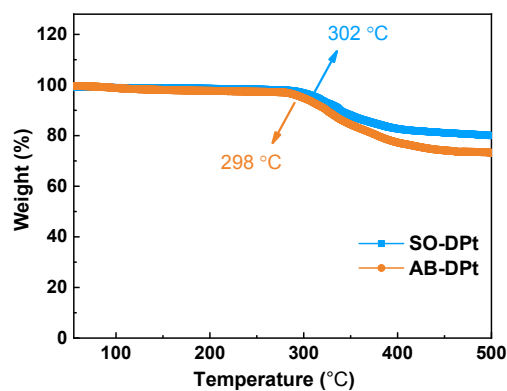


**Fig. S3** TGA curves of SO-DPt and AB-DPt.

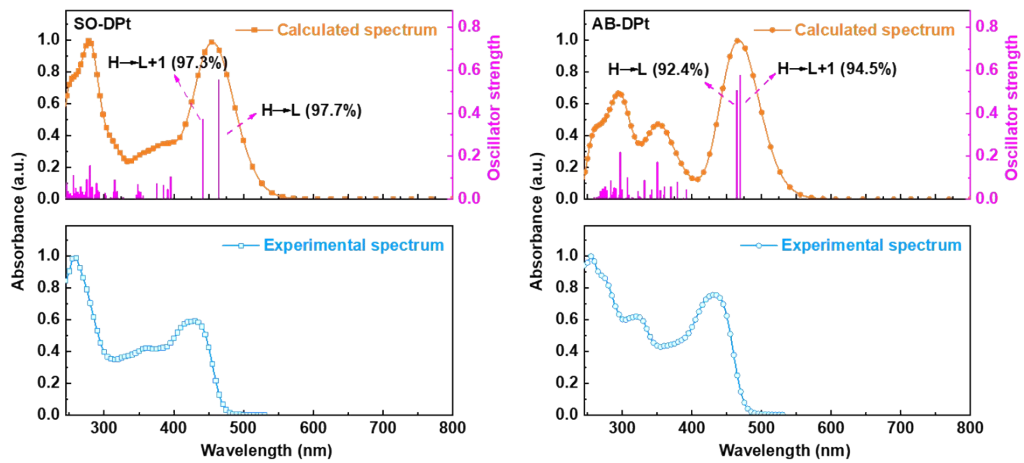


**Fig. S4** Calculation results of absorptions for **SO-DPt** and **AB-DPt**.

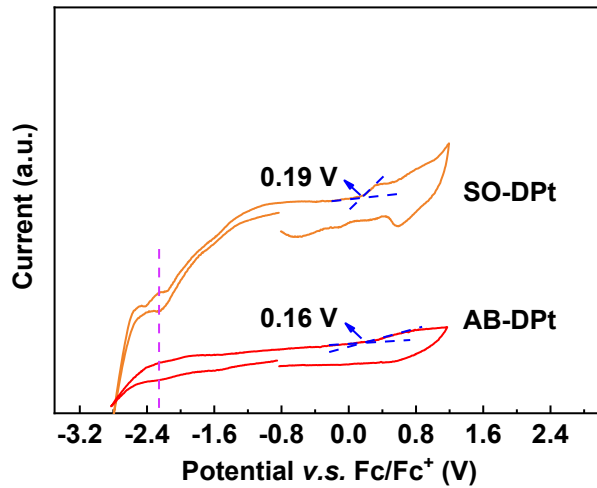


**Fig. S5** CV curves of **SO-DPt** and **AB-DPt**.

**Table S1** NTO results for **SO-DPt** and **AB-DPt**

NTOs	Contribution from Pt and ligands to MOs (%)		
	Pt	L-SO	acac
<b>SO-DPt</b>	Pt	L-SO	acac
	Particle	4.62	94.65
<b>AB-DPt</b>	Hole	3.87	95.71
	Pt	L-AB	acac
<b>AB-DPt</b>	Particle	4.61	94.66
	Hole	3.52	96.08

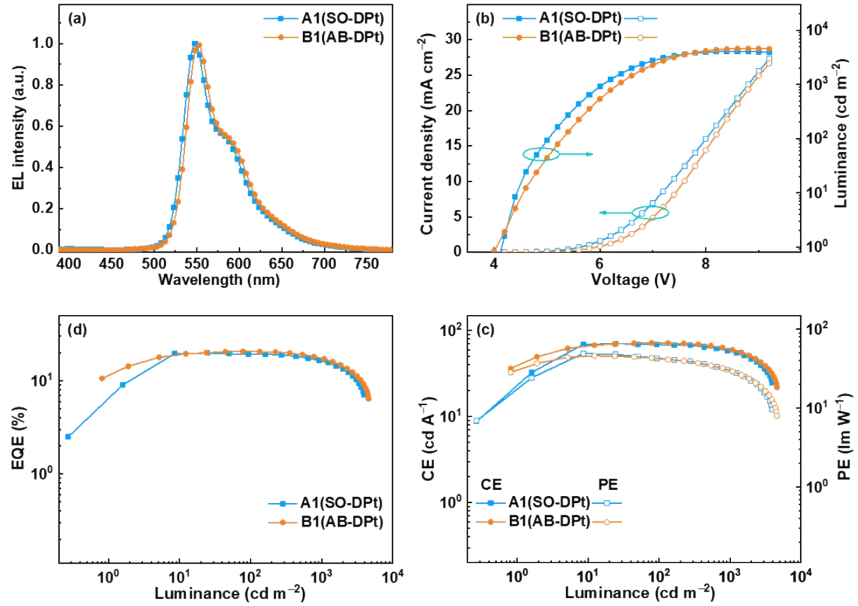


**Fig. S6** EL performance of devices A1 and B1: (a) EL spectra, (b)  $J$ - $V$ - $L$  characteristics, (c) CE/PE vs luminance, and (d) EQE vs luminance.

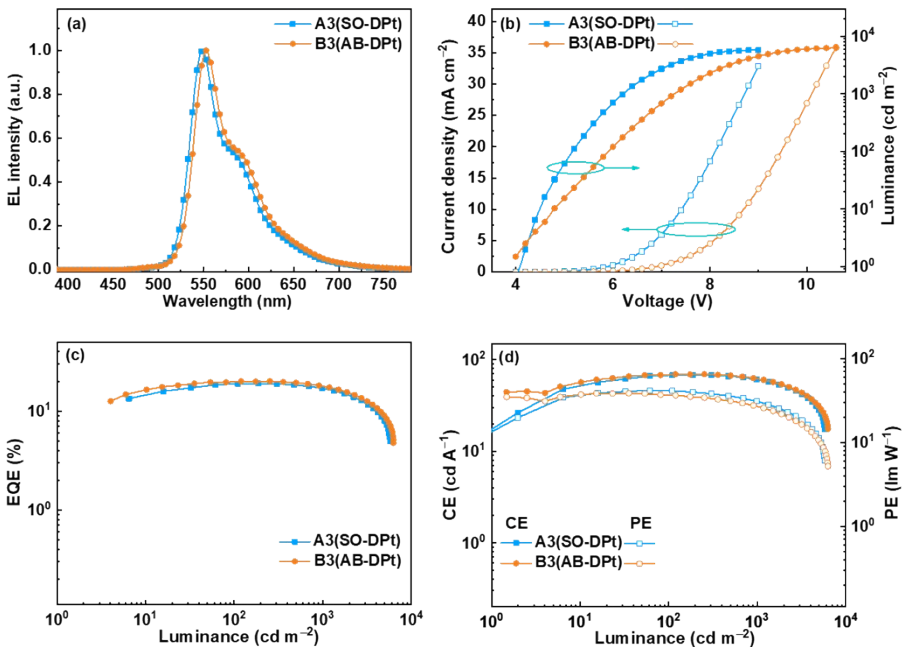


**Fig. S7** EL performance of devices A3 and B3: (a) EL spectra, (b)  $J$ - $V$ - $L$  characteristics, (c) CE/PE vs luminance, and (d) EQE vs luminance.

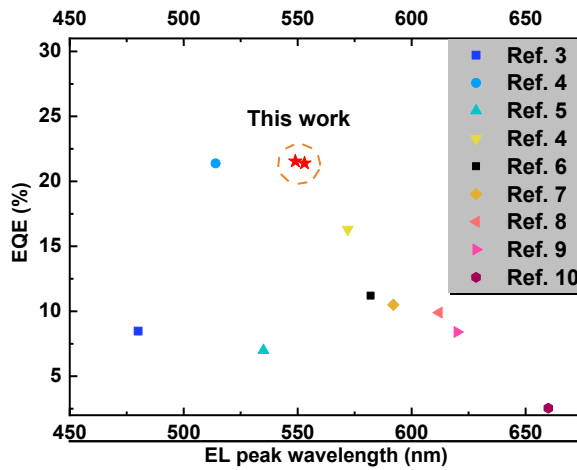


**Fig. S8** Summary of EQEs vs EL peaks of OLEDs based on dinuclear Pt(II) complexes.<sup>3-10</sup>

**Table S2** EL performance of highly efficient solution-processed yellow OLEDs

Complex	Center metal	$\lambda_{EL}$ (nm)	EQE <sub>max</sub> (%)	CE <sub>max</sub> (cd/A)	PE <sub>max</sub> (lm/W)	CIE (x, y)	Reference
SO-DPt	Pt	549	21.54	76.64	52.33	(0.43, 0.56)	This work
AB-DPt	Pt	553	21.39	74.35	48.08	(0.45, 0.54)	This work
2-FBNO	Ir	- <sup>a</sup>	18.9 <sup>b</sup>	65.7 <sup>b</sup>	64.4 <sup>b</sup>	(0.45, 0.54)	11
Complex 4	Pt	550	7.2	7.5	24.0	(0.41, 0.57)	12
Y1	Ir	578	7.55	15.1	- <sup>a</sup>	(0.53, 0.45)	13
Ir(SFXpy) <sub>3</sub>	Ir	542	12.1	46.2	36.3	(0.45, 0.54)	14
BPyPmIr	Ir	568	18.7	62.8	60.9	- <sup>a</sup>	15
Ir(TPABPBI) <sub>2</sub> (acac)	Ir	568	15.0	30.0	6.80	(0.507, 0.486)	16
FCF3BNO	Ir	- <sup>a</sup>	22.7 <sup>c</sup>	82.5 <sup>c</sup>	49.2 <sup>c</sup>	(0.43, 0.56)	17
m-LIrpic	Ir	572	17.1	43.9	23.0	(0.528, 0.469)	18
(Et-Cz-BTz)2Ir(EO2-pic)	Ir	~550	19	60	- <sup>a</sup>	(0.467, 0.524)	19
Complex 1	Ir	570	19.20	40.10	- <sup>a</sup>	(0.493, 0.500)	20
PO-01	Ir	564	23 <sup>b</sup>	71 <sup>b</sup>	72 <sup>b</sup>	- <sup>a</sup>	21
Ir(FP) <sub>3</sub>	Ir	- <sup>a</sup>	12.7	41.7	12.5	- <sup>a</sup>	22
IrST-3F	Ir	580	12.3	27.5	17.3	(0.57, 0.43)	23
PyTPt	Pt	557	16.92	56.74	29.09	(0.47, 0.52)	24

<sup>a</sup> Not reported. <sup>b</sup> Recorded at a luminance of 100 cd m<sup>-2</sup>. <sup>c</sup> Recorded at a luminance of 1000 cd m<sup>-2</sup>.

## Reference

- 1 X. Yang, X. Xu, J. Zhao, J.-s. Dang, Z. Huang, X. Yan, G. Zhou and D. Wang, Phosphorescent Platinum (II) Complexes Bearing 2-Vinylpyridine-type Ligands: Synthesis, Electrochemical and Photophysical Properties, and Tuning of Electrophosphorescent Behavior by Main-Group Moieties, *Inorg. Chem.*, 2014, **53**, 12986-13000.
- 2 J. Zhao, Z. Feng, D. Zhong, X. Yang, Y. Wu, G. Zhou and Z. Wu, Cyclometalated Platinum Complexes with Aggregation-Induced Phosphorescence Emission Behavior and Highly Efficient Electroluminescent Ability, *Chem. Mater.*, 2018, **30**, 929-946.
- 3 A. Tronnier and T. Strassner, (C<sup>4</sup>C<sup>4</sup>) Cyclometalated binuclear N-heterocyclic biscarbene platinum(II) complexes-highly emissive phosphorescent emitters, *Dalton Trans.*, 2013, **42**, 9847-9851.
- 4 Z. Hao, K. Zhang, K. Chen, P. Wang, Z. Lu, W. Zhu and Y. Liu, More efficient spin-orbit coupling: adjusting the ligand field strength to the second metal ion in asymmetric binuclear platinum(II) configurations, *Dalton Trans.*, 2020, **49**, 8722-8733.
- 5 B. Ma, P. I. Djurovich, S. Garon, B. Alleyne and M. E. Thompson, Platinum Binuclear Complexes as Phosphorescent Dopants for Monochromatic and White Organic Light-Emitting Diodes, *Adv. Funct. Mater.*, 2006, **16**, 2438-2446.

6 Y. Sun, C. Chen, B. Liu, Y. Guo, Z. Feng, G. Zhou, Z. Chen and X. Yang, Efficient dinuclear Pt(II) complexes based on the triphenylphosphine oxide scaffold for high performance solution-processed OLEDs, *J. Mater. Chem. C*, 2021, **9**.

7 X. Yang, B. Jiao, J.-S. Dang, Y. Sun, Y. Wu, G. Zhou and W.-Y. Wong, Achieving High-Performance Solution-Processed Orange OLEDs with the Phosphorescent Cyclometalated Trinuclear Pt(II) Complex, *ACS Appl. Mater. Interfaces*, 2018, **10**, 10227-10235.

8 M. Z. Shafikov, R. Daniels, P. Pander, F. B. Dias, J. A. G. Williams and V. N. Kozhevnikov, Dinuclear Design of a Pt(II) Complex Affording Highly Efficient Red Emission: Photophysical Properties and Application in Solution-Processible OLEDs, *ACS Appl. Mater. Interfaces*, 2019, **11**, 8182-8193.

9 J. Yu, X. Wu, H. Tan, Y. Liu, Y. Wang, M. Zhu and W. Zhu, High-efficiency saturated red emission from binuclear cyclo-metallated platinum complex containing 5-(4-octyloxyphenyl)-1,3,4-oxadiazole-2-thiol ancillary ligand in PLEDs, *Sci. China Chem.*, 2013, **56**, 1137.

10 J. Zhang, L. Wang, A. Zhong, G. Huang, F. Wu, D. Li, M. Teng, J. Wang and D. Han, Deep red PhOLED from dimeric salophen Platinum(II) complexes, *Dyes Pigm.*, 2019, **162**, 590-598.

11 J.-H. Jou, Y.-X. Lin, S.-H. Peng, C.-J. Li, Y.-M. Yang, C.-L. Chin, J.-J. Shyue, S.-S. Sun, M. Lee, C.-T. Chen, M.-C. Liu, C.-C. Chen, G.-Y. Chen, J.-H. Wu, C.-H. Li, C.-F. Sung, M.-J. Lee and J.-P. Hu, Highly Efficient Yellow Organic Light

Emitting Diode with a Novel Wet- and Dry-Process Feasible Iridium Complex

Emitter, *Adv. Funct. Mater.*, 2014, **24**, 555-562.

12 A. K.-W. Chan, M. Ng, Y.-C. Wong, M.-Y. Chan, W.-T. Wong and V. W.-W. Yam, Synthesis and characterization of luminescent cyclometalated platinum(II) complexes with tunable emissive colors and studies of their application in organic memories and organic light-emitting devices, *J. Am. Chem. Soc.*, 2017, **139**, 10750-10761.

13 A. Liang, G. Huang, S. Dong, X. Zheng, J. Zhu, Z. Wang, W. Wu, J. Zhang and F. Huang, Novel iridium complexes as yellow phosphorescent emitters for single-layer yellow and white polymer light-emitting diodes, *J. Mater. Chem. C*, 2016, **4**, 6626-6633.

14 B.-Y. Ren, R.-D. Guo, D.-K. Zhong, C.-J. Ou, G. Xiong, X.-H. Zhao, Y.-G. Sun, M. Jurow, J. Kang, Y. Zhao, S.-B. Li, L.-X. You, L.-W. Wang, Y. Liu and W. Huang, A Yellow-Emitting Homoleptic Iridium(III) Complex Constructed from a Multifunctional Spiro Ligand for Highly Efficient Phosphorescent Organic Light-Emitting Diodes, *Inorg. Chem.*, 2017, **56**, 8397-8407.

15 X. Yang, Z. Feng, J. Dang, Y. Sun, G. Zhou and W.-Y. Wong, High performance solution-processed organic yellow light-emitting devices and fluoride ion sensors based on a versatile phosphorescent Ir(III) complex, *Mater. Chem. Front.*, 2019, **3**, 376-384.

16 X. Ouyang, D. Chen, S. Zeng, X. Zhang, S. Su and Z. Ge, Highly efficient and solution-processed iridium complex for single-layer yellow electrophosphorescent diodes, *J. Mater. Chem.*, 2012, **22**, 23005-23011.

17 J.-H. Jou, S.-C. Fu, C.-C. An, J.-J. Shyue, C.-L. Chin and Z.-K. He, High efficiency yellow organic light-emitting diodes with a solution-process feasible iridium based emitter, *J. Mater. Chem. C*, 2017, **5**, 5478-5486.

18 G. Sarada, J. Yoon, W. Cho, M. Cho, D. W. Cho, S. O. Kang, Y. Nam, J. Y. Lee and S.-H. Jin, Substituent position engineering of diphenylquinoline-based Ir(III) complexes for efficient orange and white PhOLEDs with high color stability/low efficiency roll-off using a solution-processed emission layer, *J. Mater. Chem. C*, 2016, **4**, 113-120.

19 T. Giridhar, W. Cho, Y.-H. Kim, T.-H. Han, T.-W. Lee and S.-H. Jin, A systematic identification of efficiency enrichment between thiazole and benzothiazole based yellow iridium(III) complexes, *J. Mater. Chem. C*, 2014, **2**, 9398-9405.

20 L. Fu, M. Pan, Y. H. Li, H. B. Wu, H. P. Wang, C. Yan, K. Li, S. C. Wei, Z. Wang and C. Y. Su, A butterfly-like yellow luminescent Ir(III) complex and its application in highly efficient polymer light-emitting devices, *J. Mater. Chem.*, 2012, **22**, 22496-22500.

21 J. H. Jou, H. H. Yu, Y. X. Lin, J. R. Tseng, S. H. Peng, Y. C. Jou, C. H. Lin, S. M. Shen, C. Y. Hsieh, M. K. Wei, D. H. Lin, C. C. Wang, C. C. Chen, F. C. Tung, S. H. Chen and Y. S. Wang, High efficiency yellow organic light emitting diodes

with a balanced carrier injection co-host structure, *J. Mater. Chem. C*, 2013, **1**, 5110-5115.

22 T. Ye, S. Shao, J. Chen, L. Wang and D. Ma, Efficient Phosphorescent Polymer Yellow-Light-Emitting Diodes Based on Solution-Processed Small Molecular Electron Transporting Layer, *ACS Appl. Mater. Interfaces*, 2011, **3**, 410-416.

23 J. Zhao, X. Chen, J. Wu, M. Jian, G. Zhou and Z. Chi, Fluoro-benzenesulfonyl-functionalized 2-phenylthiazole-type iridium(III) complexes for efficient solution-processed organic light-emitting diodes, *J. Mater. Chem. C*, 2020, **8**, 10390-10400.

24 Y. Sun, B. Liu, Y. Guo, Z. Feng, G. Zhou, Z. Chen and X. Yang, Triphenylamine-based trinuclear Pt(II) complexes for solution-processed OLEDs displaying efficient pure yellow and red emissions, *Org. Electron.*, 2021, **91**, 106101.